Nucleation density from isotropic and self-nucleated melts of isotactic polystyrene: an overview from the molten to a glassy state

Mamun, Al; Ghanbari, Abbas; Nofar, Mohammadreza

Publisher's version / Version de l'éditeur:
https://doi.org/10.1134/S0965545X23600333
Polymer Science, Series A, 2024-09-16

`

Nucleation density from isotropic and self-nucleated melts of isotactic polystyrene: an overview from the molten to a glassy state

Al Mamun (https://orcid.org/0000-0002-9500-9483)[a,*], Abbas Ghanbari (https://orcid.org/0000-0002-2842-5268)[b], and Mohammadreza Nofar (https://orcid.org/0000-0002-4364-2930)[c]

[a] *Department of Physics, College of Science, University of Hafr Al Batin, Al Jamiah, Hafr Al Batin 39524, Saudi Arabia.*

[b] *National Research Council Canada, 2690 Red Fife Rd, Rosser, MB, Canada R0H 1E0.*

[c] *Sustainable & Green Plastics Laboratory, Metallurgical & Materials Engineering Department, Faculty of Chemical and Metallurgical Engineering, Istanbul Technical University, Istanbul, 34469 Turkey*

**e-mail: almamun@uhb.edu.sa*

Abstract— Nucleation density is a fundamental parameter influencing the microstructure, properties, and performance of polymeric materials. Controlling and manipulating nucleation density allows for tailoring polymeric materials with specific characteristics, enabling advancements in various fields of industrial applications. The present study investigates nucleation density from an isotropic and self-nucleated melt of isotactic polystyrene (iPS). A wide range of temperatures, from 225 to 260 °C are considered, and the samples are subjected to partial or isotropic melt followed by isothermal crystallization. In the case of partial melting below 230 °C, the nucleation density is attributed to the seed nuclei originating from self-nucleated melts due to incomplete crystal melting. Crystallization from isotropic melts involves a limited number of heterogeneous nucleation sites activated on the surfaces, impurities, or foreign particles within the melt. On the other hand, crystallization from the glassy state was found to rely on the molecular conformation and mobility in the amorphous phase, which plays a crucial role in achieving an optimal nucleation density. The experimental findings indicate that in molten and glassy states, the predetermined active nucleus sites significantly influence the nucleation process during crystallization. The nucleation density directly affects the crystallization kinetics and morphology of crystals. A higher nucleation density leads to a more significant number of smaller crystals, resulting in a finer microstructure. This can have significant implications for polymer properties such as mechanical strength, optical transparency, electrical conductivity, permeability, and thermal properties.

Keywords: isotactic polystyrene; nucleation density; isotropic melt; self-nucleated melt; glassy states

`

INTRODUCTION

Polymer crystallization encompasses nucleation and growth processes [1, 2]. Primary nuclei form from the melt phase during nucleation and transition into a three-dimensional solid phase. These primary nuclei can sporadically develop at random sites in the isotropic melt or on foreign bodies such as impurity particles, polymerization catalysts, or substrate surfaces, acting as nucleation centers [3]. Homogeneous nucleation occurs when polymer molecules spontaneously aggregate to form a three-dimensional nucleus, which must reach a critical size below the melting point. Beyond this critical size, nucleation occurs sporadically, but it does not provide definitive evidence for the homogeneous process. Heterogeneous nucleation involves activating a limited number of sites, either instantaneously or sporadically [4, 5].

During the crystallization process, the nucleation density exhibits an induction time characterized by the sporadic appearance of nucleation sites. Subsequently, the number of nucleation sites steadily increases until reaching saturation, depending on the experimental conditions. The induction time represents the period required to form a critical nucleus and often relies on the crystallization conditions. Directly observing nucleation sites using standard methods is challenging due to their small size. Therefore, small spherulites are assumed to originate from active individual nucleation sites and are observed after a certain induction time. While polymer molecule aggregation is reversible until the critical nucleus size is reached, beyond that size, an embryo larger than the critical size becomes stable, and the number of nucleation sites linearly increases over time. The number of nuclei saturates at a constant value before impinging on each other [6, 7]. The saturated nucleation density, N_s, refers to the number of sites observed per unit area, which is significantly higher in the case of homogeneous nucleation [8].

The nucleation density dramatically affects the rate of polymer crystallization. A higher nucleation density leads to faster completion of crystallization, while a lower nucleation density prolongs the process. Regarding crystallization temperature, for a system undergoing crystallization at a constant cooling rate, samples crystallized at higher temperatures have lower nucleation density compared to those crystallized at lower temperatures. This influences the lamellar thickness of the crystals, which in turn governs the ultimate melting point [8].

Amorphous glassy states of polymers are thermodynamically unstable, and their structures tend to relax toward equilibrium [9]. Annealing below the glass transition temperature (T_g) significantly impacts the thermodynamic properties [10, 11]. Numerous studies have focused on achieving thermodynamic equilibrium in the glass states of polymeric materials [10-14]. The annealing time (t_a) and temperature (T_a) influence the relaxation process. Another factor that affects

the relaxation process is the degree of crystallinity (χ_c), which can alter the state of the amorphous phase.

Our previous research investigated the nucleation and growth behavior of isotactic polystyrene (iPS) across a broad temperature range [6, 7]. In this article, we present our findings regarding the impact of annealing conditions and the nature of the melt states on nucleation density. We provide an overview of the saturated nucleation densities at various temperatures. Furthermore, we explore the dependency of the saturated nucleation density on different experimental conditions during the crystallization process of iPS.

EXPERIMENTAL

Idemitsu Kosan Co. Ltd. supplied isotactic polystyrene (iPS) with high tacticity. The polymer has a molecular weight of M_w=17800 and M_n=10600, with a narrow molecular weight distribution (M_w/M_n =1.67). The equilibrium melting temperature of this iPS was previously determined to be 242 °C [7]. To ensure the removal of any previous remnant residue, the sample was melted and crystallized five times. The crystallization and melting behavior were investigated using a Shimadzu TA 60 instrument, following a specified heating and cooling rate for a typical experiment.

Thermogravimetric analysis was conducted under a nitrogen atmosphere using a Q60-SDT thermal analysis (TA) instrument. Approximately 5 mg of the iPS sample was degraded entirely by heating from room temperature to 600 °C at 10 °C/min. Differential scanning calorimetry (DSC) measurements were performed using a TA instrument Q2000 DSC, where an empty aluminum pan was the reference. The DSC instrument was calibrated before measurements using high-purity standard indium with a melting point of 156.6 °C. All DSC measurements were conducted at a heating rate of 10 °C/min, and the typical sample weight was 3 ± 0.1 mg. To prevent thermal degradation, the sample pan was surrounded by nitrogen gas.

A Zeiss Axioscop polarizing optical microscope was utilized for imaging purposes, capturing images of melt press films placed on a Linkam hot stage equipped with a temperature controller and cooling unit. Photomicrographs were recorded using a Toshiba HV-D27 3CCD camera and analyzed using Image-Pro Plus 4.0 software. The saturated nucleation density was determined by counting the number of small spherulites per unit volume of the sample in the real-time images observed through the optical microscope.

`

RESULTS AND DISCUSSION

Polymeric materials usually thermally degrade if they melt far above their melting temperatures. To mitigate the risk of thermal degradation, an initial evaluation was conducted to assess the thermal stability of isotactic polystyrene (iPS). The thermogravimetric tests were conducted for temperatures ranging from 20 to 600 °C at a heating rate of 10 °C/min. Figure 1 illustrates the residual mass (TGA) and the mass-loss rate (DTG) within the designated temperature range of 100 to 500 °C for convenience. The TGA and DTG curves exhibit a single-stage degradation process characterized by a single peak. The figure indicates that degradation begins at 340 °C, the maximum mass loss rate is observed at 414 °C, and complete mass loss occurs at 465 °C. As a result, it is deemed safe to melt iPS up to a maximum temperature of 260 °C for a short duration, as long as it falls between the equilibrium melt temperature (reported as 242 °C [15] and later verified by us [7]) and the observed degradation temperature. Any melting above the equilibrium melting temperature of 242 °C will be considered an isotropic melt.

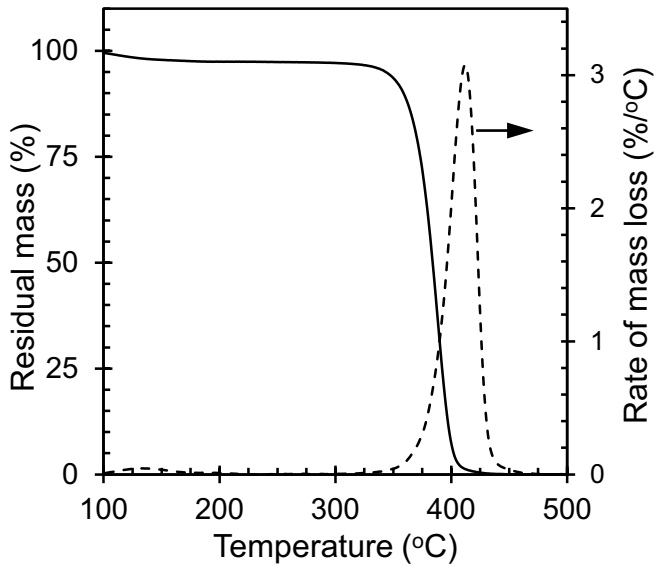

Figure 1. Thermograms for the residual mass (solid curve for primary axis) and the mass loss rate (broken curve for secondary axis) against temperature for iPS.

To estimate the range of glass temperature, crystallization-recrystallization temperature, and melt temperatures for the studied iPS, a conventional DSC scan was conducted on the crystallized sample. Before the DSC heating scan at a rate of 5 °C/min, the sample was initially melted from the isotropic melt state at 250 °C and subsequently crystallized at 160 °C for 8 hours. The temperature profile leading up to the DSC heating scan is presented in Figure S1 in the accompanying document. Figure 2 illustrates the relationship between DSC heat flow and

`

temperature. This plot shows a region corresponding to the glass temperature between 77-90 °C. An exothermic peak is evident at approximately 195 °C, attributed to the recrystallization process during the heating scan. Two endothermic peaks representing melting events are observed in the 204-228 °C temperature range. It was confirmed that the lower melting point increases linearly with the crystallization temperature, exhibiting a slope of approximately 0.5 according to the Hoffman-Weeks plot [16]. This relationship yields an equilibrium melting temperature of 242 °C.

Conversely, the higher melting point remains relatively unaffected by the crystallization temperature. The higher melting peak can be explained by the melting of rearranged lamellae (thickening) during DSC heating [17]. For iPS with the specified molecular weight, melting beyond the equilibrium temperature of 242 °C is considered an isotropic melt. Based on the DSC data, the temperatures can be categorized into three regions: the glass temperature region (T_g), the crystallization-recrystallization temperature region (T_c), and the melting temperature region (T_f). Within the melting temperature region, subcategories can be identified, including the insufficient melting region (T_{f1}), the melting region (T_{f2}), and the isotropic melting region above 242 °C (T_{f3}), as depicted in Figure 2.

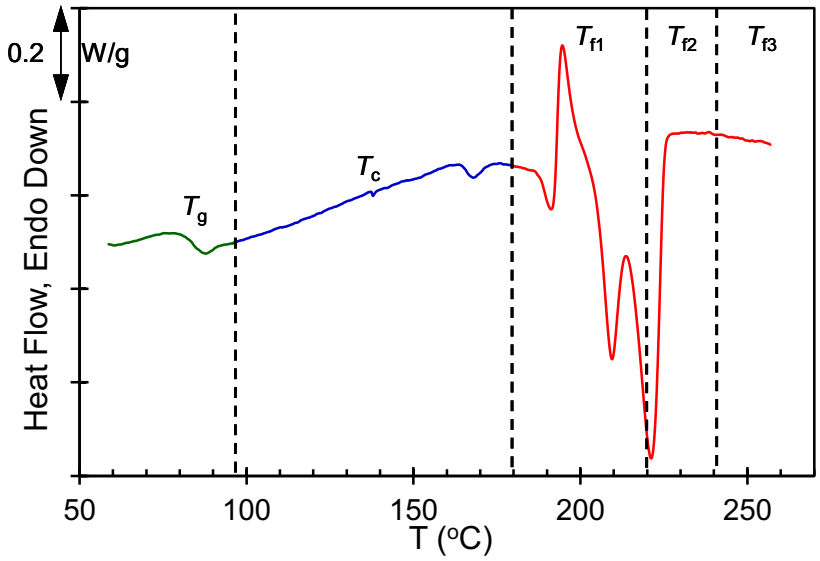

Figure 2. Plot of the heat flow against temperature of isothermally crystallized iPS with a heating rate of 5 °C/min. The sample was melted from the isotropic melt at 250 °C before crystallization and then was kept at 160 °C for 8 hours.

Figure 3a depicts the temperature profile for the nucleation density with time from the isotropic melt under the conditions specified in the temperature profile. The samples were melted at 250 °C and subsequently annealed at the indicated temperature for five minutes before isothermally crystallizing at 160 °C. The time-dependent nucleation density shows sporadic behavior as a function of annealing temperature. The nucleation behavior exhibits a time-dependent pattern,

`

commencing with an induction period, followed by sporadic emergence of small spherulites. As time progresses, the number of spherulites (N) increases until it reaches a maximum value. This maximum value, known as the saturated nucleation density (N_s), remains constant until the completion of crystallization. Direct observation of crystal nuclei poses challenges due to their small size. Therefore, small spherulites are assumed to initiate from active individual sites and become observable only after a certain induction period. During this period, the aggregation of polymer molecules is reversible until a critical size is reached. Beyond this critical size, a nucleus larger than the critical size continues to grow steadily, resulting in a linear increase in the number of nuclei with time.

Consequently, the saturated nucleation density is estimated based on the saturated number of nuclei per unit volume, with the initial volume under the optical microscope serving as the reference for determining the nominal nucleation density. The induction time represents the duration required for critical nucleus formation and is commonly used to measure the primary nucleation rate. The total number of nuclei is restricted to a constant value (N_s) until the crystallization process is completed. This saturated nucleation behavior has been observed in several polymers [7, 18]. It should be noted that the residual melt region still accounts for approximately 90% of the system, and the limiting values observed are not attributed to a reduced space available for nucleation, such as impingement among spherulites.

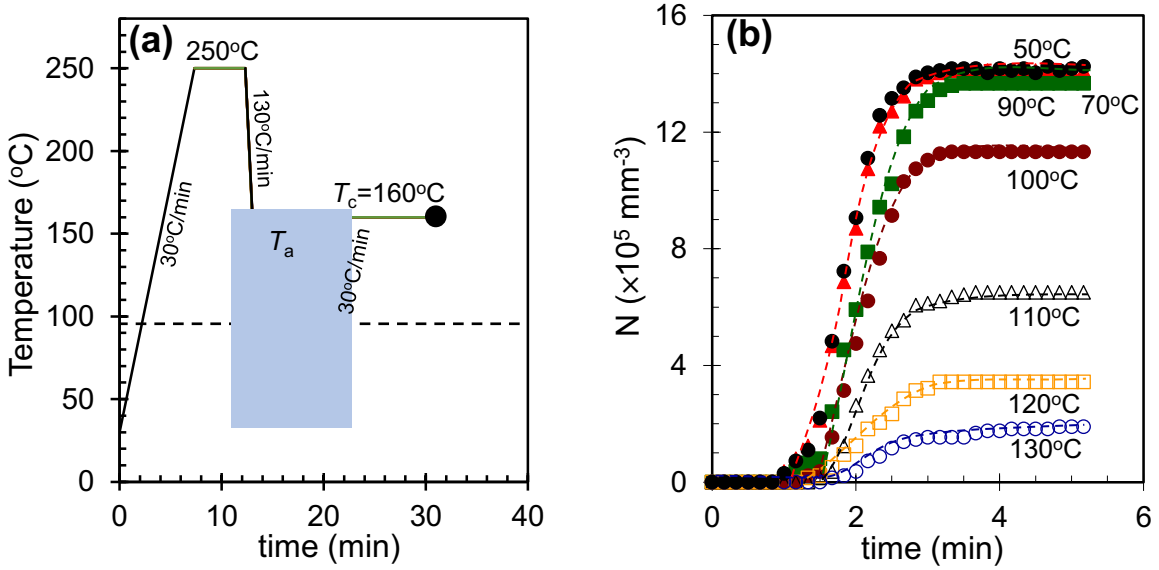

Figure 3. (a) Temperature profile for the nucleation density with time from the isotropic melt, and (b) Number of nuclei (N) increases with time as a function of annealing temperatures (T_a) as indicated in the figure. Samples were melted at 250 °C and subsequently annealed at the indicated temperature for five minutes before isothermally crystallizing at 160 °C.

`

When the sample was subjected to a crystallization temperature of 160 °C (T_c) for a short period (t_{c1}) following the melting of the isotropic melt at 250 °C (T_{f3}), the crystallization process was promptly halted after the spherulites had grown to only a few microns in size. Subsequently, the sample was melted at T_{f2}, for instance, 230 °C for 5 minutes, and then subjected to crystallization at the same temperature of 160 °C, following the procedure depicted in Figure 4. This particular sample, which underwent the procedure above, is referred to as "type A" and exhibits partial crystallization, where the growth of spherulites is arrested before reaching sizes greater than a few microns. Notably, the spherulites reappeared at the exact locations, indicating that the substrate surface influences the nucleation of spherulites. The limited size attained by the spherulites, as shown in Figure 4, is attributed to the slow crystal growth rate in iPS. When the crystallization was terminated before the spherulites grew beyond a few microns in size from the molten state at T_{f3}, the saturated nucleation density remained unaffected by T_{f2} temperatures above 225 °C.

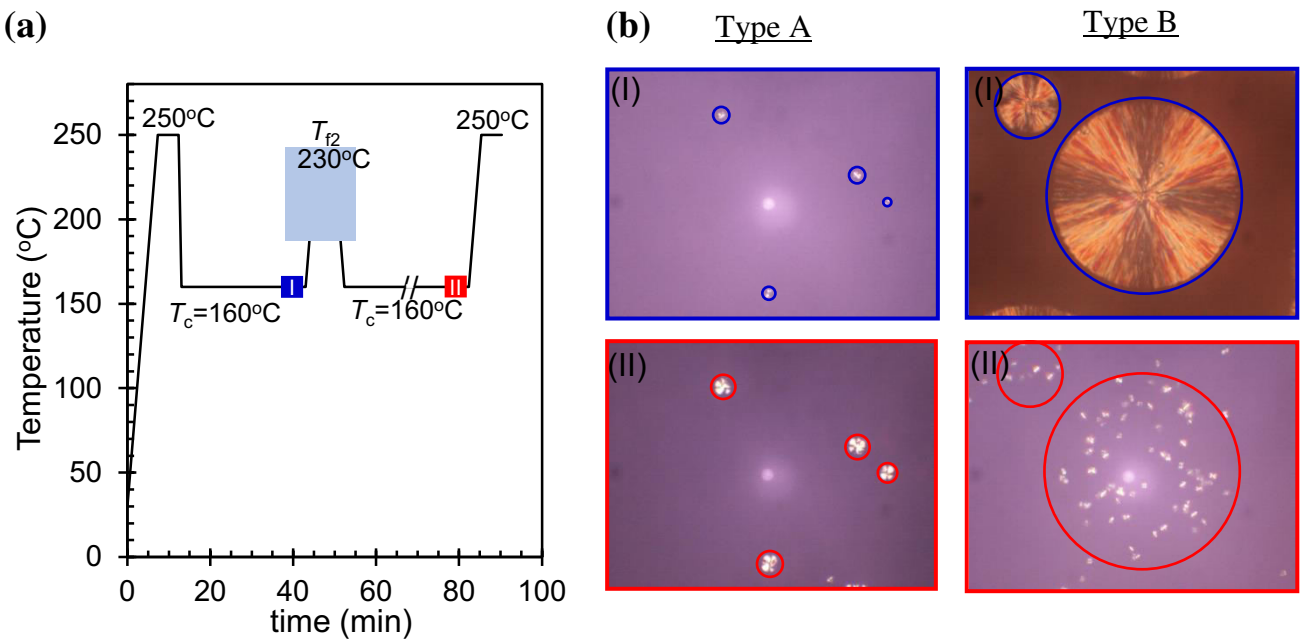

Figure 4. (a) Temperature profile to study the effect of melt temperature on saturated nucleation density, and (b) The optical micrographs of spherulites crystallized at 160 °C; from the melt at 250 °C (T_{f3}) for a time of ten minutes (t_{c1}) within the critical size (left images), and exceeding the critical spherulite's size for a time of two hours (t_{c1}) (right images). The size of each image is 200µm×150µm.

At 250 °C (T_{f3}), any remnant residues from previous crystallizations were effectively eliminated. The crystallization conditions at t_{c1} and T_c controlled the size of the spherulites. Figure 4 illustrates the spherulites that grew during this period (t_{c1}). Subsequently, the crystallized sample was melted at 230 °C (T_{f2}) for 5 minutes following the procedure outlined in Figure 4. The

`

spherulites with controlled sizes are referred to as “original spherulites,” and the sample crystallized under these conditions is designated “type B”, demonstrating partial crystallization based on spherulite size. When the sample is crystallized at 160 °C from the melt at 230 °C (T_{f2}), numerous small spherulites with a granular structure emerge within the outline of the original spherulite, as observed in Figure 4. This occurrence of small spherulites within the original spherulite is a phenomenon previously observed for many polymers [19-22]. These small spherulites are believed to result from inadequate melting of the crystal structure within the original spherulite. These surviving crystal structures are nucleation sites due to a self-seeding effect during subsequent crystallization. The self-seeding effect, caused by incomplete crystal melting, is widely recognized and referred to as a memory effect. The previous melting temperature, duration, and size of the original spherulite strongly influence the number of sites induced by self-nucleation.

Interestingly, the nucleation density appears somewhat higher at the boundary of the original spherulite than at its interior. Several factors could contribute to this phenomenon, including the concentration of impurities or molecular fractionation at the boundary layer during crystallization. Additionally, the boundary might have a thermal effect during reheating and crystallization. However, the nucleation density is nearly homogeneous when the sample is completely crystallized. Approximately 90% of the melt regions persist until the nucleation density reaches saturation.

Furthermore, it can be anticipated that the nucleation rate is higher at the center than at the boundary of the original spherulite, as the rate increases with an elevation in molecular weight [23]. Thus, the findings depicted in Figure 4 are not attributed to molecular fractionation. These outcomes imply that the thermal history at the boundary influences nucleation during subsequent remelting and crystallization processes. In addition, the thermal history can induce lamellar thickening at the boundary layer, thereby enhancing the memory effect in the original spherulite. However, the specific reasons for forming the concentric structure remain unclear.

Figure 5 illustrates the correlation between the size of the original spherulite and the number of small spherulites (additional induced nucleation sites) within the original spherulite domain. As the size of the original spherulite increases, the number of additional nucleation sites also increases. However, the rate of increment of nucleation sites decreases as the melt temperature (T_{f2}) increases. A critical size of the crystallite nucleus of the original spherulite has been identified at which the newly induced nucleation sites start to appear. The critical size of the crystallite nucleus of the original spherulite expands with higher melt temperatures, as depicted in the inset of Figure 5. This critical size can be estimated based on the growth rate (G) of the spherulite, the induction time

`

(τ_o), and the transition time (t_o) at which the additional nuclei begin to emerge within the original spherulites. Notably, the transition time increases as the melt temperature rises, as shown in the inset of Figure 5.

Interestingly, the spacing between the nucleation sites aligns with the diameter of the critical spherulite. A similar phenomenon related to crystallinity has been observed in nylon-6, where the nucleation mechanism shifts from sporadic nucleation to instantaneous nucleation at approximately 15% degree of crystallinity. Additionally, the overall crystallization rate accelerates with higher initial degrees of crystallinity [25].

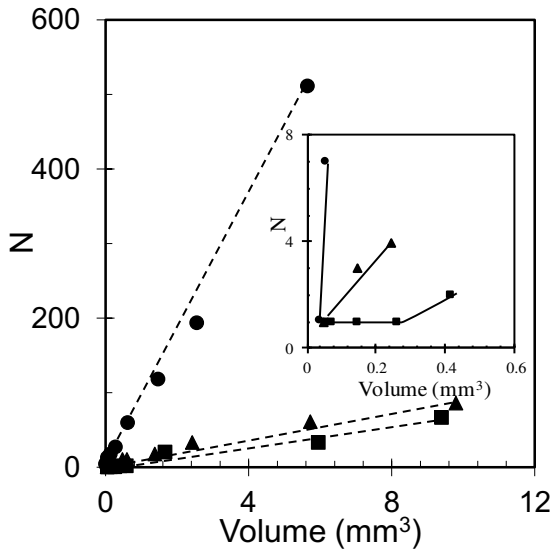

Figure 5. Plots of the number of nuclei (type B) as a function of the volume of the original spherulite (the volume was calculated by the observed area under POM and by the thickness of the sample) crystallized from the melt at three different temperatures (T_{f2}): 230 (square), 228 (triangle), and 225 °C (circle). The inset presents the early nucleation stages and denotes the transition time at which additional nuclei begin to appear in the original spherulites.

The original spherulites were grown at 160 °C (T_{f3}) from the melt until they reached complete crystallization by impinging upon each other. The temperature profile illustrated in Figure S2 was followed for this experiment. This completely crystallized sample was then melted at 230 °C (T_{f2}) and subjected to another round of crystallization at 160 °C. This fully crystallized sample prepared under these conditions is called "type C", representing complete crystallization. The saturated nucleation density (N_s) for type C was measured and plotted against the melt temperature (T_{f2}) in Figure 6, alongside the saturation density for type A. It can be observed that the saturation density for type C significantly increases by several thousand as the melt temperature decreases from 250 to 225 °C, whereas the saturation density for type A remains constant. Conversely, nearly identical results are obtained when the melt temperature is increased from 225 to 250 °C, as depicted

`

in Figure 6. The change in saturation density from type A to type C is strongly influenced by the size of the original spherulite, similar to the case of type B. A larger spherulite size leads to a much higher value for the number of saturated nuclei until the original spherulites impinge upon each other. These additional nucleation sites result from inadequate melting of the original spherulite. The nucleation behavior described above follows a sigmoidal curve characterized by the sporadic appearance of nuclei and a limited number of nuclei. These limited nucleation sites arise from incompletely melting the original crystal structure, which induces nucleation sites through a self-seeding effect during subsequent crystallization. This self-seeding nucleation process is likely associated with the distribution of cluster sizes or embryos formed from crystal fragments originating from the incomplete melting of crystals. Hence, the spherulite formation mechanism can be discussed in the following way. It is generally accepted that after a nucleus (several folds of chains) reaches a critical size, it grows to form lamellar crystallite. The presence of this crystallite limits the amount of conformations available to the nearby chains, and secondary nucleation occurs. Such chain reaction of secondary nucleation results in the growth of spherulite, where lamellar crystallites are divided by amorphous regions composed of loops, tie chains and cilia. Obviously, not all crystallites within the spherulite are the same. They may vary in terms of thickness, other lateral dimensions, number of defects, number of tie chains that connect one lamellae to another (stressed state) etc. Obviously, the variation of these properties affects the thermal stability of a crystallite. The most stressed, defective and small crystallites will melt at lower temperatures, while the most perfect and probably thickest crystallites will melt last. If some (the most stable crystallites) did not melt after annealing at T_{f2}, they will become nuclei for new spherulites after cooling. And, even if all the crystallites fully melted, chains that have been a part of the most stable crystallites (which have melted last) had less time to “forget” their previous conformation and are thus more prone to fold again to form the nucleus.

`

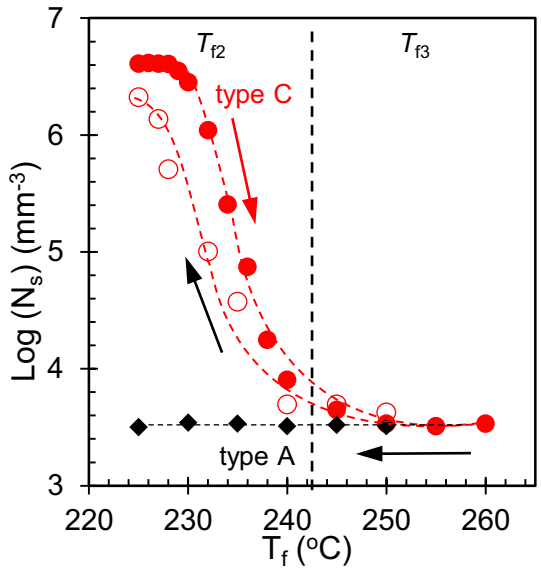

Figure 6. Relationship between the saturated nucleation density (N_s) and melt temperature (T_f) for type C: complete crystallization, samples were isothermally crystallized at 160 °C by changing the melt temperature (T_f) from lower to higher (solid circle) and from higher to lower (open circle), and type A: partial crystallization below the critical size (solid diamond).

The impact of annealing on nucleation density was further investigated at lower temperatures. In this study, the sample was melted from the isotropic melt, rapidly cooled to a specific annealing temperature, and then subjected to isothermal crystallization at 160 °C. It was observed that the nucleation density increases as the annealing temperature decreases until reaching the glass temperature regions, as depicted in Figure 7. However, below the glass temperatures, the nucleation density reaches a constant value. These findings suggest that during the rapid quenching process to lower temperatures, the conformation of the amorphous state, which tends to relax, might be responsible for the observed increase in saturated nucleation densities.

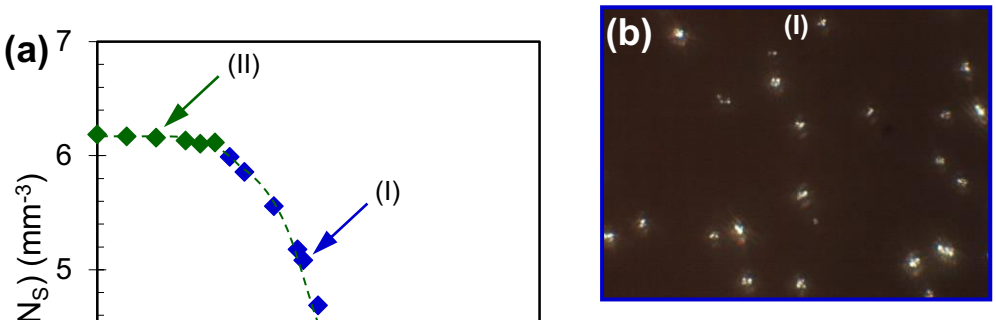

`

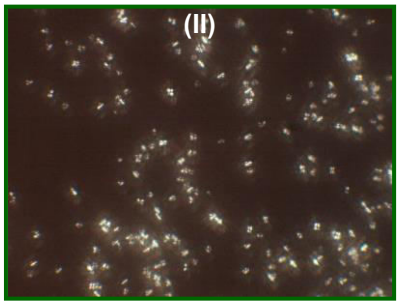

Figure 7. (a) Plots of the saturation density (N_s) as a function of the temperature (T_a), and (b) the corresponding optical micrographs as indicated by arrows. The sample was melted at isotropic melt and rapidly cooled to the corresponding temperature before further isothermal crystallization at 160 °C. The size of each image is 200μm×150μm.

A series of experiments were conducted to investigate the impact of annealing on nucleation density. Initially, the sample was partially crystallized at 160 °C from the isotropic melt at 250 °C. It was then rapidly cooled to a specific temperature and held for five minutes before undergoing further crystallization at 160 °C. Figure S3 in the supporting information depicts this process's temperature profile. Upon examining Figure 8, it is evident that during the initial crystallization stage, only a few small spherulites can be observed (circled in the corresponding optical images in Figure I), with notable errors in the calculation. However, a surprising increase in nucleation density was observed after rapid quenching to the glassy state.

Furthermore, the existing spherulites became more visible in the optical microscopy image (Figure 8bII). The nucleation density increased as the annealing temperature decreased, reaching a constant value below the glass transition temperature. This increase confirms the quenching effect on the sample.

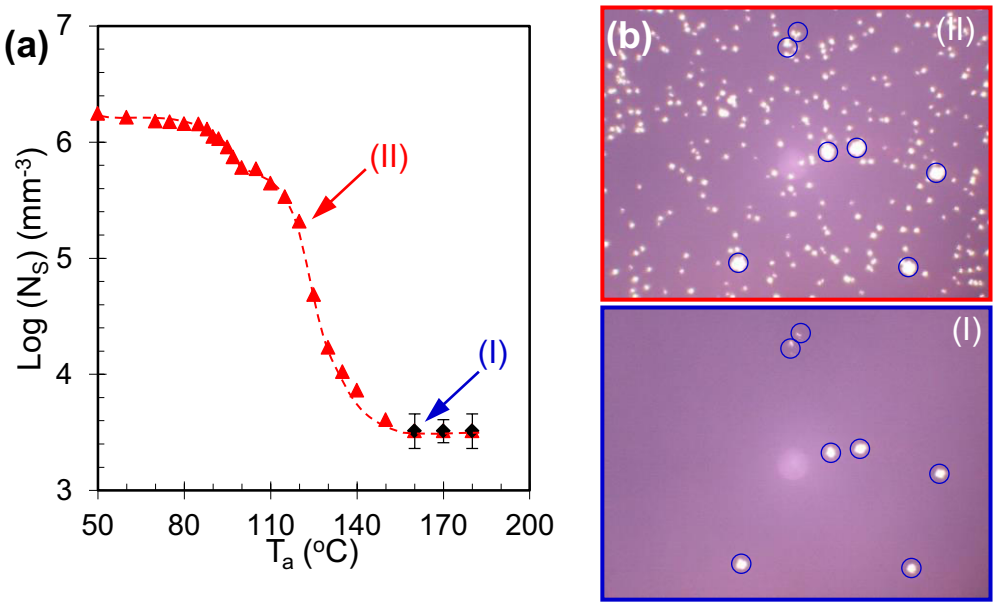

`

Figure 8. (a) Plots of the saturation density (N_s) as a function of the temperature (T_a), and (b) the corresponding optical micrographs as indicated by arrows. The sample was crystallized isothermally from isotropic melt (solid diamond) and then quenched to the corresponding temperature before further isothermal crystallization (solid triangle) at 160 °C. The size of each image is 200μm×150μm.

Figure 9 compares the DSC heat flow and observed nucleation density across a wide temperature range, encompassing all regions. A strong correlation is observed between the saturated nucleation densities with isotropic and self-nucleated melts. In the glass temperature region, characterized by the conformation of the polymer chain in the glassy amorphous fraction prior to crystallization, a consistently high and constant nucleation density is observed. The annealing conditions (t_c and T_c) in the crystallization-recrystallization temperature region greatly influence the saturated nucleation density in this region. In the melting temperature region, a critical spherulite size is identified, beyond which induced nucleation sites begin to emerge within the original spherulite's outline during subsequent crystallization. When the crystallization process is halted before reaching this critical spherulite size, the nucleation behavior exhibits no dependence on the melting temperature.

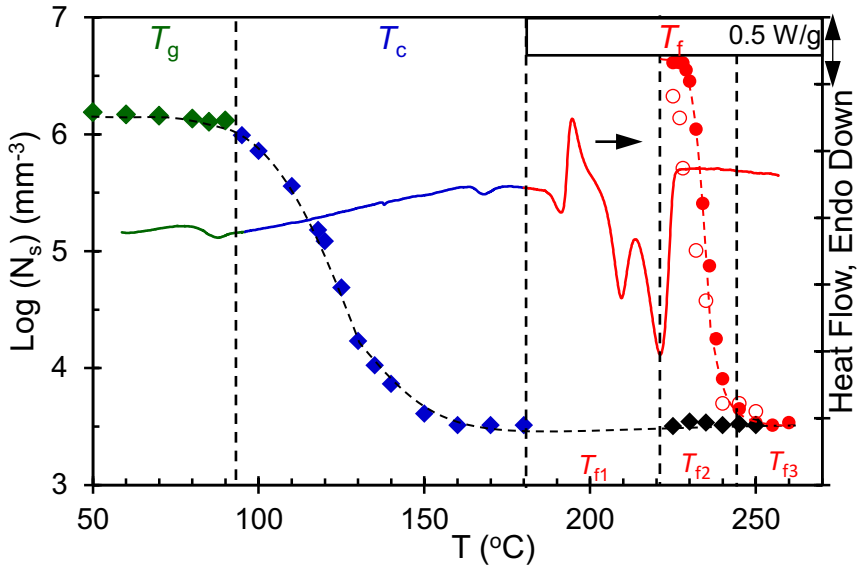

Figure 9. Plots of the saturated nucleation density (N_s) and DSC heat flow as a function of temperature correlate the different temperature regions of nucleation density with heat flow.

However, when the spherulites grew larger than the critical spherulite size, a phenomenon occurred where numerous small spherulites in a granular structure emerged within the boundaries of the original spherulite during subsequent crystallization. The number of additional nucleation sites within the granular structure increased with the original spherulite size, while the increase in nucleation sites reduced with higher T_{f1}. These granular structures were likely a result of inadequate

melting of the crystal structure within the original spherulite, leading to the induction of nucleation sites through a self-seeding effect during subsequent crystallization. The saturated nucleation density (N_s) substantially increased by several thousand as T_{f2} decreased from 250 to 225 °C.

CONCLUSIONS

A comprehensive investigation explored the impact of isotropic and self-nucleated melts on the nucleation density of isotactic polystyrene. The nature of the molten state was found to influence the nucleation sites prior to crystallization significantly. When crystallization occurred from a heterogeneous melt, the nucleation density was primarily attributed to seed nuclei resulting from self-nucleated melts, which arose from the incomplete melting of the spherulites. This led to a remarkably high nucleation density compared to crystallization from isotropic melts. On the other hand, in the case of crystallization from a homogeneous melt, only a limited number of nucleation sites persisted, typically activated on the surfaces of impurities or foreign particles within the isotropic melt.

Furthermore, the initial size of the spherulites before melting played a crucial role in further amplifying the nucleation density. The crystallization process, starting from the glassy state, exhibited significant influence from the molecular conformation and mobility within the amorphous phase, thereby promoting a higher nucleation density. The nucleation density remained constant below the glass transition temperature because the maximum number of active nucleation sites was activated in the amorphous melt before crystallization.

ACKNOWLEDGMENT

The author thanks Dr. Susumu Umemoto, Department of Organic and Polymeric Materials, Tokyo Institute of Technology, Tokyo, Japan, for his fruitful discussion during manuscript preparation. The author is also grateful to the Mechanical Engineering Department and the Deanship of Scientific Research, University of Hafr Al Batin, Saudi Arabia, for their gracious permission to use their experimental facilities.

SUPPORTING INFORMATION

Information is available regarding the temperature profile for crystallization at 160 °C for 8 hours from the isotropic melt prior to the DSC experiment, as shown in Figure S1. In addition, the temperature profile is shown to study the saturated nucleation density as a function of melting

`

temperature and annealing temperature, as shown in Figure S2 and Figure S3, respectively. Supporting information can be obtained from the Online Library or from the author.

`

REFERENCES

[1] Y. Long, R.A. Shanks, Z.H. Stachurski, Kinetics of polymer crystallisation, Progress in Polymer Science 20(4) (1995) 651-701.
[2] A. Thierry, C. Straupé, J.-C. Wittmann, B. Lotz, Organogelators and Polymer Crystallisation, Macromolecular Symposia 241(1) (2006) 103-110.
[3] F.L. Binsbergen, Natural and artificial heterogeneous nucleation in polymer crystallization, Journal of Polymer Science: Polymer Symposia 59(1) (1977) 11-29.
[4] Y.-L. Loo, R.A. Register, A.J. Ryan, G.T. Dee, Polymer Crystallization Confined in One, Two, or Three Dimensions, Macromolecules 34(26) (2001) 8968-8977.
[5] L. Sangroniz, D. Cavallo, A.J. Müller, Self-Nucleation Effects on Polymer Crystallization, Macromolecules 53(12) (2020) 4581-4604.
[6] A. Mamun, S. Umemoto, N. Ishihara, N. Okui, Influence of thermal history on primary nucleation and crystal growth rates of isotactic polystyrene, Polymer 47(15) (2006) 5531-5537.
[7] A. Mamun, S. Umemoto, N. Okui, N. Ishihara, Self-Seeding Effect on Primary Nucleation of Isotactic Polystyrene, Macromolecules 40(17) (2007) 6296-6303.
[8] K.A. Narh, J.A. Odell, A. Keller, G.V. Fraser, The effect of nucleation density on the kinetics of crystallization and on the resulting structure and thermal properties of polymers crystallized during cooling, Journal of Materials Science 15(8) (1980) 2001-2009.
[9] V.P. Privalko, S.S. Demchenko, Y.S. Lipatov, Structure-dependent enthalpy relaxation at the glass transition of polystyrenes, Macromolecules 19(3) (1986) 901-904.
[10] R.M. Syamaladevi, G.V. Barbosa-Cánovas, S.J. Schmidt, S.S. Sablani, Influence of molecular weight on enthalpy relaxation and fragility of amorphous carbohydrates, Carbohydrate Polymers 88(1) (2012) 223-231.
[11] W. Sakatsuji, T. Konishi, Y. Miyamoto, Effects of thermal history on enthalpy relaxation, Journal of Thermal Analysis and Calorimetry 113(3) (2013) 1129-1134.
[12] Y.S. Lipatov, V.P. Privalko, S.S. Demchenko, Y.D. Besklubenko, G.V. Titov, V.F. Shumskii, The structural "memory" of amorphous polystyrene, Polymer Science U.S.S.R. 28(3) (1986) 639-646.
[13] T.M. Murphy, D.S. Langhe, M. Ponting, E. Baer, B.D. Freeman, D.R. Paul, Enthalpy recovery and structural relaxation in layered glassy polymer films, Polymer 53(18) (2012) 4002-4009.
[14] X. Liu, W. Yu, Role of chain dynamics in the melt memory effect of crystallization, Macromolecules 53(18) (2020) 7887-7898.
[15] A.P.T. Pezzin, G.O.R. Alberda van Ekenstein, E.A.R. Duek, Melt behaviour, crystallinity and morphology of poly(p-dioxanone), Polymer 42(19) (2001) 8303-8306.
[16] J.D. Hoffman, J.J. Weeks, Melting process and the equilibrium melting temperature of polychlorotrifluoroethylene, J. Res. Natl. Bur. Stand., Sect. A 66(1) (1962) 13-28.
[17] T. Liu, Melting behavior of isotactic polystyrene revealed by differential scanning calorimetry and transmission electron microscopy, European Polymer Journal 39(7) (2003) 1311-1317.
[18] P. Supaphol, J.E. Spruiell, Crystalline memory effects in isothermal crystallization of syndiotactic polypropylene, Journal of Applied Polymer Science 75(3) (2000) 337-346.
[19] Y. Ohta, H. Murase, T. Hashimoto, Effects of spinning conditions on the mechanical properties of ultrahigh-molecular-weight polyethylene fibers, Journal of Polymer Science Part B: Polymer Physics 43(19) (2005) 2639-2652.
[20] N. Okui, S. Umemoto, R. Kawano, A. Mamun, Temperature and Molecular Weight Dependencies of Polymer Crystallization, in: G. Reiter, G.R. Strobl (Eds.), Progress in Understanding of Polymer Crystallization, Springer Berlin Heidelberg, Berlin, Heidelberg, 2007, pp. 391-425.
[21] B. Wang, R. Utzeri, M. Castellano, P. Stagnaro, A.J. Müller, D. Cavallo, Heterogeneous Nucleation and Self-Nucleation of Isotactic Polypropylene Microdroplets in Immiscible Blends:

`

From Nucleation to Growth-Dominated Crystallization, Macromolecules 53(14) (2020) 5980-5991.
[22] J. Li, Z. Jiang, Z. Qiu, Isothermal melt crystallization kinetics study of cellulose nanocrystals nucleated biodegradable Poly(ethylene succinate), Polymer 227 (2021) 123869.
[23] S. Umemoto, R. Hayashi, R. Kawano, T. Kikutani, N. Okui, Molecular Weight Dependence of Primary Nucleation Rate of Poly(Ethylene Succinate), Journal of Macromolecular Science, Part B 42(3-4) (2003) 421-430.

`

Supporting Information

Nucleation density from isotropic and self-nucleated melts of isotactic polystyrene: an overview from the molten to a glassy state

Al Mamun (https://orcid.org/0000-0002-9500-9483)[a,*], Abbas Ghanbari (https://orcid.org/0000-0002-2842-5268)[b], and Mohammadreza Nofar (https://orcid.org/0000-0002-4364-2930)[c]

[a] *Department of Physics, College of Science, University of Hafr Al Batin, Al Jamiah, Hafr Al Batin 39524, Saudi Arabia.*

[b] *National Research Council Canada, 2690 Red Fife Rd, Rosser, MB, Canada R0H 1E0.*

[c] *Sustainable & Green Plastics Laboratory, Metallurgical & Materials Engineering Department, Faculty of Chemical and Metallurgical Engineering, Istanbul Technical University, Istanbul, 34469 Turkey*

**e-mail: almamun@uhb.edu.sa*

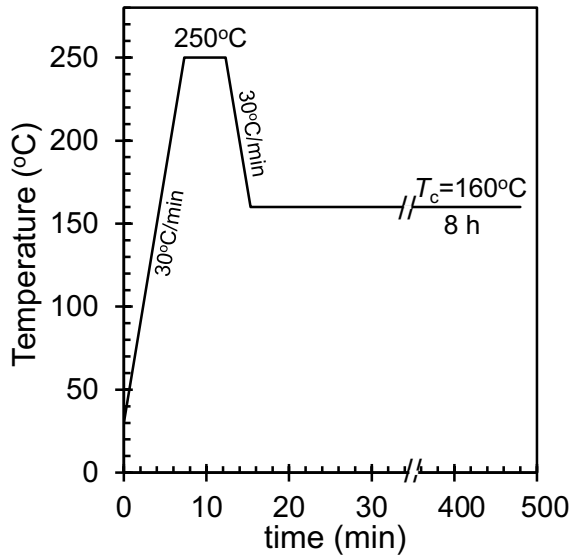

Figure S1. The temperature profile for crystallization at 160 °C for 8 hours from the isotropic melt prior to the DSC experiment is shown in Figure 2.

`

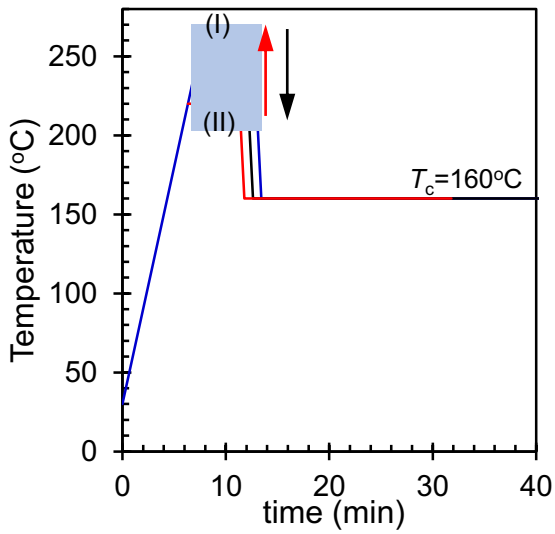

Figure S2. Temperature profile to study the saturated nucleation density as a function of melting temperatures. The sample was melted at higher temperatures and then completely crystallized at 160 °C. Afterward, it melted at relatively higher or lower temperatures (type C). The sample was melted at higher temperatures and then crystallized for an insufficient time at 160 C. Afterward, it melted at relatively lower temperatures (type A).

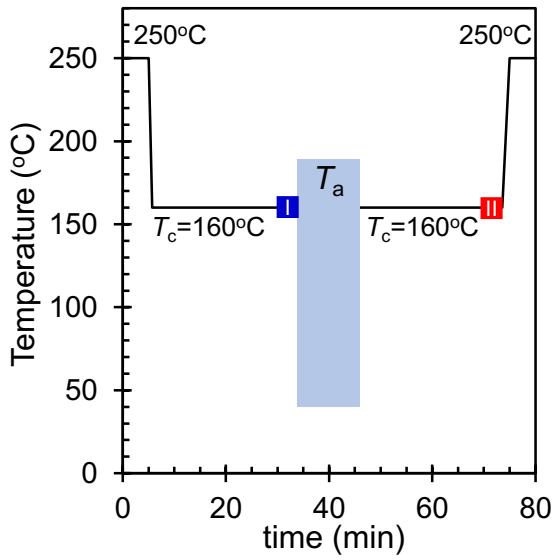

Figure S3. Temperature profile to study the saturated nucleation density as a function of annealing temperatures.

`

Graphical Abstract

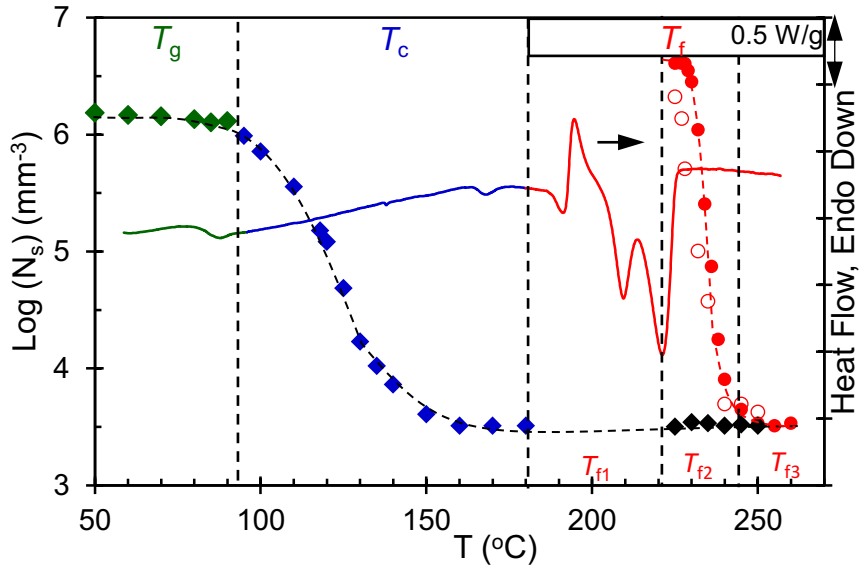

FUNDING

No funding information is available for this article.

CONFLICT OF INTEREST

The authors declare that they have no conflicts of interest.